Proc. Natl. Acad. Sci. USA
Vol. 87, pp. 6482–6486, September 1990
Biochemistry

Analytical determination of receptor–ligand dissociation constants of two populations of receptors from displacement curves

(binding/cyanopindolol)

HAGAI ALMAGOR† AND ALEXANDER LEVITZKI‡

†The Fritz Haber Research Center for Molecular Dynamics and ‡Department of Biological Chemistry, Institute of Life Sciences, The Hebrew University of Jerusalem, Jerusalem, Israel 91904

Communicated by Terrell L. Hill, May 24, 1990 (received for review December 21, 1989)

ABSTRACT **The determination of receptor–ligand dissociation constants from displacement data has been restricted until recently to the condition of receptor saturation, in which the concentration of receptor is negligible as compared to the displaced ligand and the displacing ligand used. This restriction has lately been removed since an accurate method has been developed for the determination of the dissociation constants for all experimental conditions for a system that includes a single type of binding site. In many cases, however, there are two types of receptor binding sites that exhibit different affinities toward the ligand. The present study provides an analytic solution for the problem of determination of the two dissociation constants as well as the proportion of the two receptor types. The formal derivation of the equations is described, along with analysis of a displacement simulation. The sensitivity of the method to the ratio between the two dissociation constants is also investigated. The application of the method is demonstrated for the analysis of the binding of β-adrenergic receptors to the agonist isoproterenol as monitored by the displacement of the β-antagonist ^{125}I-labeled cyanopindolol.**

Receptor–ligand dissociation constants can sometimes be determined by directly measuring ligand binding to the receptor. However, ligand binding affinity is often too low to be measured directly, usually because of the high dissociation rate of the ligand–receptor complex. This results in a half-life of the complex too short for successful trapping on a filter (see ref. 1 for review). Methods other than filtration are technically cumbersome and usually require impractically large amounts of the receptor, which is accessible in limited quantities. It has therefore become a routine procedure to measure the dissociation constant of low-affinity ligands by their displacement of another high-affinity ligand from the receptor. For the simple interpretation of the ligand displacement curve, Cheng and Prusoff (2) had to make the assumption that the displaced ligand is in large excess over the receptor, implying that the free ligand concentration remains equal to its total concentration throughout the displacement experiment. It is also assumed that the concentration of the displacing ligand is much higher than that of the receptor sites. Moreover, the treatment of Cheng and Prusoff is limited to the case of one class of receptor sites. Recently, Horovitz and Levitzki (3) have developed an analytical method to analyze ligand displacement curves for an assumption-free case, waiving the preconditions necessary for the validity of the Cheng–Prusoff equation.

The Cheng–Prusoff treatment and the Horovitz–Levitzki improvement deal with one class of binding sites that exhibits a single affinity. In this communication we describe a method for analysis of the displacement of radioactive ligand from a mixed population of two types of binding sites that exhibit different dissociation constants. In the treatment to follow we arrive at an assumption-free analytical solution that is valid for all experimental conditions.

The publication costs of this article were defrayed in part by page charge payment. This article must therefore be hereby marked "*advertisement*" in accordance with 18 U.S.C. §1734 solely to indicate this fact.

Theory

Table 1 summarizes all of the parameters used in the following derivation. The aim of the derivation is to correlate L, the amount of radioactive ligand bound, with H_t, the total concentration of added nonradioactive displacing ligand, such that K_a and K_b and the fraction of each population, α and $\bar{\alpha}$, can be accurately obtained. The system consists of a population of two types of binding sites: a and b. The radioactive ligand, L, exhibits a dissociation constant, K_L, that is identical to both types of sites. The nonradioactive displacing ligand, H, exhibits a dissociation constant, K_α, to a fraction (α) of sites of type a and a dissociation constant, K_b, to a fraction ($1 - \alpha$) of sites of type b.

The fraction of sites occupied by radioactive ligand, Y, is given by

$$Y = \frac{XL}{2R_t}.$$

By definition the dissociation constant is given by

$$K_L = \frac{x \cdot L}{XL}.$$

Concentration of free sites is given by

$$x = 2R_t - \sigma - 2R_t \cdot Y.$$

The concentration of free radioactive ligand is given by

$$L = L_t - XL = L_t - 2R_t \cdot Y.$$

Hence,

$$K_L = \frac{x \cdot (L_t - 2R_t \cdot Y)}{2R_t \cdot Y},$$

and therefore

$$x = \frac{2R_t \cdot Y \cdot K_L}{L_t - 2R_t \cdot Y}. \qquad [1]$$

The concentration of free sites is expressed as a function of Y only in Eq. 1. The concentration of free displacing ligand, h, is

$$h = H_t - \sigma$$

while

Table 1. Parameters used in derivation of equations

h	Concentration of free displacing ligand
H_t	Total concentration of displacing ligand
$2R_t$	Total concentration of binding sites
α	Fraction of sites of type "a"
$\bar{\alpha} \equiv (1 - \alpha)$	Fraction of sites of type "b"
L	Concentration of free radioactive ligand
L_t	Total concentration of radioactive ligand
X_a	Concentration of free sites of type "a"
X_b	Concentration of free sites of type "b"
$x \equiv X_a + X_b$	Concentration of free sites
XL	Concentration of bound radioactive ligand
H_a	Concentration of nonradioactive displacing ligand bound to "a" type sites
H_b	Concentration of nonradioactive displacing ligand bound to "b" type sites
$\sigma \equiv H_a + H_b$	Total concentration of bound displacing ligand
$\bar{\sigma} \equiv 2R_t - \sigma$	Concentration of receptor sites not occupied by displacing ligand
K_L	Dissociation constant of radioactive ligand from either site
K_a	Dissociation constant of nonradioactive displacing ligand from site "a"
K_b	Dissociation constant of nonradioactive displacing ligand from site "b"
Y	Fraction of sites occupied by radioactive ligand

$$\sigma = 2R_t - XL - x$$

$$= 2R_t - 2R_t \cdot Y - x$$

or

$$\sigma = 2R_t(1 - Y) - x, \qquad [2]$$

and thus

$$h = H_t - 2R_t(1 - Y) + x. \qquad [3]$$

The concentration of free displacing ligand is given by Eq. 3 (with Eq. 1) as a function of Y only.

Derivation of Linear Equations

The fraction of sites not bound to displacing ligand is given by $\frac{\alpha \cdot 2R_t - H_a}{2R_t - \sigma}$ and $\frac{\bar{\alpha} \cdot 2R_t - H_b}{2R_t - \sigma}$ for type a and type b sites, respectively. These proportions also hold for the two populations of sites bound to the radioactive ligand and for the free sites of the two types, since the radioactive ligand binds with equal affinity to both type a and type b sites. The concentration of free sites of each type is therefore given by

$$X_a = x \cdot \frac{\alpha 2R_t - H_a}{2R_t - \sigma}; \quad X_b = x \cdot \frac{\bar{\alpha} 2R_t - H_b}{2R_t - \sigma}. \qquad [4]$$

By the definition of the dissociation constants K_a and K_b we have

$$H_a = \frac{X_a \cdot h}{K_a}; \quad H_b = \frac{X_b \cdot h}{K_b}. \qquad [5]$$

By substituting Eq. 4 in Eq. 5 and using the definition of σ we get

$$\sigma = 2R_t xh \cdot \frac{xh + \bar{\sigma} \cdot (\alpha K_b + \bar{\alpha} K_a)}{\bar{\sigma}^2 K_a K_b + \bar{\sigma} xh \cdot (K_a + K_b) + (xh)^2}. \qquad [6]$$

Upon rearrangement and using the definitions $K^* \equiv K_a K_b$, $K^+ \equiv K_a + K_b$, $\bar{K} \equiv \alpha K_b + \bar{\alpha} K_a$ we get

$$\sigma \bar{\sigma}^2 K^* + \sigma \bar{\sigma} (xh) K^+ + \sigma (xh)^2 = 2R_t (xh)^2 + 2R_t \bar{\sigma} (xh) \bar{K}. \qquad [7]$$

Since $\sigma \neq 0$ and $\bar{\sigma} \neq 0$ we can write

$$\frac{(xh)^2 + 2R_t (xh) \bar{K}}{\sigma \bar{\sigma}} = \frac{(xh)}{\bar{\sigma}} K^+ + K^*. \qquad [8]$$

For the appropriate value of $\bar{K}$, Eq. 8 yields a linear function of $\frac{(xh)}{\bar{\sigma}}$, with K^+ as the slope and K^* as the intercept. Choosing a wrong value for $\bar{K}$ should cause the function to be convex or concave relative to the linear curve. Alternatively, the reciprocal equation can be used

$$\frac{(xh) + 2R_t \bar{K}}{\sigma} = \frac{\bar{\sigma}}{(xh)} K^* + K^+, \qquad [8a]$$

with K^* as the slope and K^+ as the intercept.

From the derivation it is apparent that the only experimental data required are (*i*) total concentration of receptor, R_t, which can be obtained by direct binding experiments using the radioactive ligand L, and (*ii*) the degree of occupancy at each concentration of the displacing ligand H. No assumptions are required concerning L_t or H_t. By varying the value of $\bar{K}$, one can find for a given set of data the proper value of $\bar{K}$ that linearizes Eq. 8 (or Eq. 8a). The values of K_a and K_b can thus be determined and, knowing $\bar{K}$, so can α.

Displacement Equation

Substituting explicitly for x, h, σ, and $\bar{\sigma}$ (using Eqs. 1–3), and performing elementary algebraic manipulations, Eq. 7 can be transformed into a polynomial (of 5th degree) in Y. The physical root of this polynomial (identified by the condition $0 \leq Y \leq 1$) describes Y as a function of H_t. One can thus reconstruct the displacement curve for any set of the parameters and variables. One can also use optimization procedures for the determination of the dissociation constants and α by optimal fit of the reconstructed displacement curve to the experimental data. Simulation of some displacement curves is presented in Fig. 1.

Analysis Simulation

In Fig. 2 a set of curves generated by Eq. 8a for different values of $\bar{K}$ is described, using the simulation of a typical displacement experiment as shown in Fig. 1*b*. Although the correct value of $\bar{K}$ generates a straight line, curves are convex for values too large or concave for values too small. The values of K_a and K_b are determined from the slope and intercept of the straight line in Fig. 2.

Resolution of Dissociation Constants

The resolution limit of the analysis depends mainly on the experimental error in the data, but it is also a function of α: the smaller the proportion of one type of sites, the harder it is to measure its dissociation constant accurately. It is useful to have an estimate of the resolution limit as a function of the population parameter α. To simulate experimental error we superimposed "noise" on the simulation curves. To each simulation value Y an error was introduced by adding a random value within the error range $\pm f \cdot E(Y)$, wherein $E(Y)$ is the statistical error range of radioactivity count for the value Y (see below), and f is a constant factor supposed to

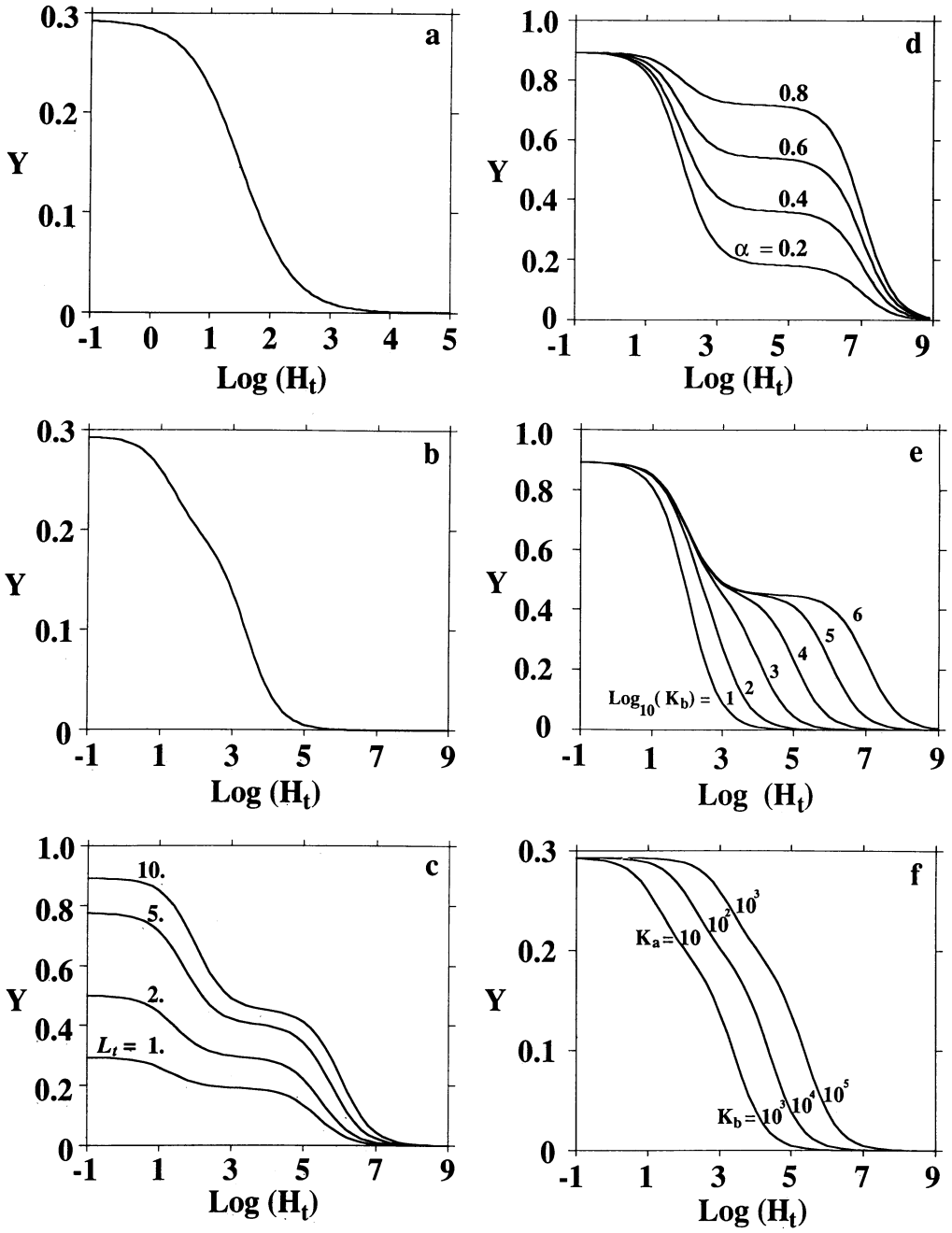

FIG. 1. Displacement curves for various sets of parameters. (*a*) System with a single class of binding site: $K_a = K_b = 10$, $K_L = R_t = L_t = 1$. The curve is sigmoidal with a single inflection point. (*b*) System with two classes of binding sites: $K_a = 10$, $K_b = 10^3$, $\alpha = 0.5$, $K_L = R_t = L_t = 1$. The curve has two sigmoidal phases with three inflection points. (*c*) Effect of varying L_t, the total concentration of the radioactive ligand, on the displacement curve. With increasing L_t, the middle inflection point converges to $Y = \bar{\alpha}$. $K_a = 10$, $K_b = 10^5$, $\alpha = 0.5$, $K_L = R_t = 1$. (*d*) Effect of varying α on the displacement curve. At large enough L_t the middle inflection point approaches the limit $Y = \bar{\alpha}$. The limit is achieved for $Y(0) = 1$—i.e., when $L_t >> 2R_t$. (*e*) The biphasic shape of the displacement curve develops gradually with increasing the difference between K_a and K_b. K_b is varied from $K_b = K_a$ to $K_b = 10^3 \cdot K_a$. Other parameter values: $K_a = 10$, $\alpha = 0.5$, $K_L = R_t = 1$, $L_t = 10$. (*f*) Effect on the displacement curve of varying K_a and K_b at constant K_a/K_b. The curve is merely shifted along the H_t abscissa with no change of its shape. The shift is proportional to the fold of change in the dissociation constant.

include all other experimental error. $E(Y)$ is calculated as follows. Suppose the background radioactivity level is b and the conversion factor from radioactivity counts to Y is c. Since background count is subtracted from total count, and since radioactive decay error range is $\sqrt{\text{counts}}$, then $E(Y)$, the radioactivity error range for the value Y, is given by

$$E(Y) = \frac{\sqrt{c \cdot Y + b} + \sqrt{b}}{c}.$$

The analysis was based on the data shown in Fig. 4, which is an experiment of very high quality in which the experimental error is as small as can be expected. The error parameters are hence $b = 778$ cpm, $c = 332{,}240$ cpm, and $f = 15$. This gives an average error of $\approx 6\%$. (For detailed experimental information see ref. 4).

The exact shape of the displacement curve is determined by the ratio K_b/K_a; changing the values of K_a and K_b without changing their ratio results in merely shifting the curve to either higher or lower range of the displacing ligand concen-

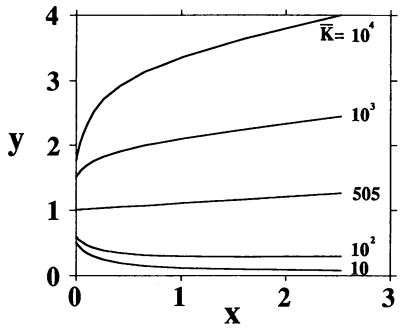

FIG. 2. Curvature analysis of simulated displacement data. Eq. **8a** was applied to the simulation data of Fig. 1*b*, using several different values for $\bar{K}$. The correct value of 505 ($K_a = 10$, $K_b = 10^3$, $\alpha = 0.5$) yields a straight line, whereas other values yield either convex or concave curves. K_a and K_b are then calculated from the intercept and slope of the straight line, as described in the text. y and x are the function $\left(\frac{(xh) + 2R_t\bar{K}}{\sigma}\right)$ and argument $\left(\frac{\bar{\sigma}}{(xh)}\right)$ of Eq. **8a**, respectively, expressed in arbitrary units. The curve of $\bar{K} = 10^4$ is actually shown divided by a factor of 6 for the aesthetics of the plot.

tration (see Fig. 1*f*). Therefore only the ratio K_b/K_a should concern us in the resolution analysis. For each α, the minimum of K_b/K_a was determined for which no simulation curve of a single site model (i.e., $K_a = K_b$) could fit the simulation "data" within the error range. (K_a was arbitrarily defined as the smaller, so $K_b/K_a \geq 1$.) That minimum ratio is taken as a measure of the resolution of dissociation constants for the given population parameter α. The resolution measure as a function of α is shown in Fig. 3.

Computer Work

All simulations and analyses were done on a CCI-POWER6 computer. IMSL FORTRAN routines ZPOLR, ZXSSQ, and RLLAV were used for polynomial solving, nonlinear regression, and linear regression, respectively. A FORTRAN program is available for the analysis of experimental data and simulation of displacement curves and can be supplied upon request.

Discussion

Displacement of a radioactively labeled antagonist from a mixed population of receptors, each displaying a different affinity, results in complex displacement curves. The composite Cheng–Prusoff equation, used to evaluate the fraction of each class of receptors and its affinity to the displacing ligand, suffers from the same disadvantage as the original Cheng–Prusoff equation—namely, it is assumed that the concentration of the displaced ligand as well as that of the displacing ligand is in excess of the concentration of the receptor. Indeed, it was pointed out (5) that the complex interactions of the β-adrenoceptor with β-agonists cannot be uncovered from ligand displacement experiments analyzed according to the conventional (6, 7) analysis. These authors (5) and others (4) have therefore used other methods for the analysis of β-adrenoceptor interaction with its agonists. In the present study we provide a general method to accurately calculate the receptor agonist dissociation constant for each of the two subpopulations comprising the total population of receptors. Ligand displacement curves depicting the behavior of a population of two classes of receptors always appear complex and are composed of two phases (e.g., Fig. 1*c*). If the two phases of the curve are well separated (e.g., in Fig. 1*e*, where $K_a/K_b = 10^{-5}$), then each phase can be appropriately described as a displacement curve of a single-site system and thus can be analyzed separately. However, generally the two phases overlap and analysis should be based rigorously on the two-site formulation. The explicit solution presented here serves this goal.

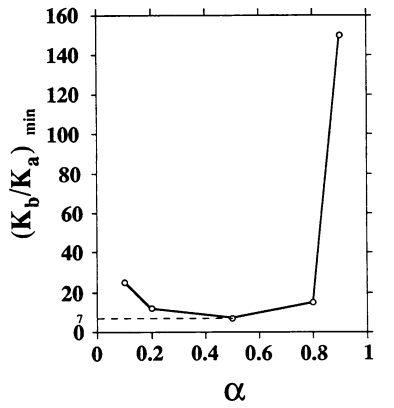

FIG. 3. Resolution of dissociation constants as a function of the population ratio. As the ratio K_b/K_a approaches 1 (K_a is arbitrarily defined as the smaller), the power of the method decreases to make the distinction between the two dissociation constants. Due to experimental noise, a single dissociation constant may in such case describe the data satisfactorily. The minimum ratio $(K_b/K_a)_{min}$ for which a single site curve fails to describe the data is shown as a function of the population ratio α. For $\alpha = 0.5$ the resolution limit is $K_b/K_a = 7$.

There are three inflection points of the displacement curve, one inflection for each phase and a middle inflection between them. If the two dissociation curves differ by several orders of magnitude then the displacement curve is horizontal at the middle inflection point and represents the end point of the titration of the sites of smaller dissociation constant (type a). In the case of one type of site all three inflection points converge to one point (e.g., the case of $K_a = K_b$ in Fig. 1*e*). The position of the middle inflection point is influenced by the population parameter, α, and by the initial saturation level, $Y(0)$. For a large $Y(0)$—i.e., when initially all sites are bound—the inflection point is at $Y = \bar{\alpha}$. However, when L_t is very small many sites are free and the displacing ligand, which initially binds to sites of higher affinity, causes the increase in the proportion of type b sites available for the radioactive ligand without changing Y much. Thus actual displacement occurs later on mainly from type b sites, and the middle inflection point occurs at Y levels close to $Y(0)$.

In principle, according to the procedure suggested in this study, one can determine the values of K_a, K_b, and α by varying $\bar{K}$ until Eq. **8** (or Eq. **8a**) describes a straight line. From the intercept and the slope of the straight line one can then calculate the three parameters, using the definitions of K^*, K^+, and $\bar{K}$. For this "curvature analysis" one needs to calculate for each experimental datum point, and for any selected $\bar{K}$, the values of the function and the argument of Eq. **8** (or Eq. **8a**). One thus gets a curve for each value of $\bar{K}$. Since the values obtained by Eq. **8** (and likewise Eq. **8a**) vary within a very wide range of numbers (a few orders of magnitude), one should only plot that part of the curve that explicitly shows the nonlinearity for wrong values of $\bar{K}$. Generally speaking, this includes in the analysis data points from that part of the displacement curve that shows the greatest change—i.e., to exclude the asymptotic parts in the beginning and in the end. In practice, however, the values of the parameters can be much improved by an additional step of parameter optimization wherein the values obtained by the curvature analysis serve as initial values. Parameter optimization of Eq. **8** (or Eq. **8a**) requires reasonably good initial values, hence the importance of the curvature analysis step. However, if the order of magnitude of the dissociation constants is known, a direct optimization of the parameters may be successful. In this case a previous knowledge of α would be of great help. α can be determined experimentally

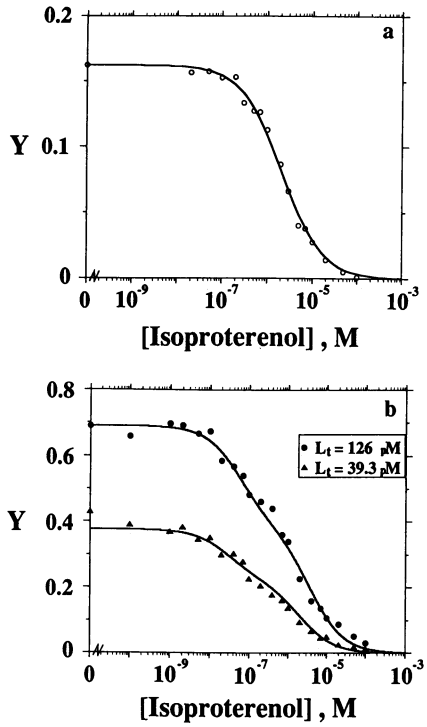

FIG. 4. Displacement by isoproterenol of ^{125}I-labeled cyanopindolol from β-adrenoceptors in (*a*) turkey erythrocyte membranes and (*b*) S49 lymphoma cell membranes. Y, the fraction of sites bound to radioactive ligand, is described as a function of the concentration of displacing ligand. [We are indebted to I. Marbach (Department of Biological Chemistry) for the data.] (*a*) Turkey erythrocyte membranes. All receptors in this membrane are believed to be in a single, high-affinity state. The displacement data are described by a single-site displacement curve, with optimized dissociation constant K_H = 4.3×10^{-7} M. The error range for K_H is $\pm 0.5 \times 10^{-7}$ M. Experimental conditions are from ref. 4. The K_d for ^{125}I-labeled cyanopindolol from direct binding was 20 pM. (*b*) S49 lymphoma cell membranes. In this membrane two states of the receptor are believed to coexist, one with low affinity and the other with high affinity to isoproterenol. Displacement data are shown for two different total concentrations of the radioactive ligand, L_t. Parameter optimization of K_a, K_b, and α was carried out for the high L_t data. The same set of optimal parameters fit both data sets: $K_a = 7.2 \times 10^{-7}$ M, K_b = 1.4×10^{-8} M, $\alpha = 0.5$. The error range of any given parameter depends on the values of the other two parameters. The value of K_a ranges from 0.6 to 1.4 μM, K_b ranges from 14 to 20 μM, and α is between 0.52 and 0.72. Experimental conditions are from ref. 4. The K_d for ^{125}I-labeled cyanopindolol from direct binding experiments was 26 pM.

using an excess of radioactive ligand (very high L_t). When all sites are initially occupied by the radioactive ligand, the middle inflection point serves as the end point of the titration of the high-affinity binding sites; at this point all high-affinity sites are replaced by nonradioactive ligand. Therefore in these conditions, $(1 - \alpha)$ equals Y at the middle inflection point.

The curvature analysis and the parameter optimization may be carried out using a computer program available from us. The total number of binding sites must be determined experimentally. The computer than estimates $\bar{K}$, K_a, and K_b, using Y values derived from displacement experiment. Examples of the application of the analysis procedure to experimental data are presented for a single-site system in Fig. 4*a* and for a two-site system in Fig. 4*b*. In the case of the two-site system, one set of data was used to get optimized values for K_a, K_b, and α. Another set of data of the same system, but with lower total concentration of radioactive ligand, was then described with the same optimized values of the parameters (Fig. 4*b*). The good fit of the same set of the parameters to both data sets demonstrates the reliability of the procedure.

When α is close to either 0 or 1 then one of the two phases of the displacement curve may be masked by experimental noise, and a single-site curve is then sufficient to fit the data. This is also the case when the ratio K_b/K_a approaches 1. Fig. 3 shows the minimum ratio that can still be detected as a function of α. The minimum ratio ranges from about 7 at α = 0.5 to about 200 at $\alpha = 0.9$ or $\alpha < 0.1$. This estimate is crude, and for some sets of the parameters (R_t, L_t, K_L) or different noise conditions a smaller limit may be achieved. However, the resolution analysis presented in Fig. 1 was based on a set of data of very high accuracy; thus the estimated resolution depends largely on the quality of the experimental data. Analysis of the displacement of ^{125}I-labeled cyanopindolol from S49 lymphoma cell membranes (Fig. 4) clearly demonstrates the power of the method described. Generally speaking, one might say then that a ratio of 1 order of magnitude between the two dissociation constants is detectable by the method.

We are grateful to Dr. I. Marbach for the experimental displacement data. This work was supported by a postdoctoral fellowship from the Scheuer Fund and by National Institutes of Health Grant GM 33710.

1. Levitzki, A. (1980) in *Cellular Receptors*, eds. Schulster, D. & Levitzki, A. (Wiley, London), pp. 9–28.
2. Cheng, Y. & Prusoff, W. M. (1973) *Biochem. Pharmacol.* **22,** 3099–3108.
3. Horovitz, A. & Levitzki, A. (1987) *Proc. Natl. Acad. Sci. USA* **84,** 6654–6658.
4. Marbach, I., Shiloach, J. & Levitzki, A. (1988) *Eur. J. Biochem.* **172,** 239–246.
5. Abramson, S. N. & Molinoff, P. B. (1985) *J. Biol. Chem.* **260,** 14580–14588.
6. Stadel, J. M., De Lean, A. & Lefkowitz, R. J. (1980) *J. Biol. Chem.* **255,** 1436–1441.
7. Wregett, K. A. & De Lean, A. (1984) *Mol. Pharmacol.* **26,** 214–227.